

**Adsorbate–Surface Phonon Interactions
in Deuterium-Passivated Si(111)-(1 × 1)**

G. A. Ferguson, and Krishnan Raghavachari David J. Michalak, and Yves Chabal

J. Phys. Chem. C, **2008**, 112 (4), 1034-1039 • DOI: 10.1021/jp0758768

Downloaded from <http://pubs.acs.org> on November 25, 2008

More About This Article

Additional resources and features associated with this article are available within the HTML version:

- Supporting Information
- Access to high resolution figures
- Links to articles and content related to this article
- Copyright permission to reproduce figures and/or text from this article

[View the Full Text HTML](#)

Adsorbate–Surface Phonon Interactions in Deuterium-Passivated Si(111)-(1 × 1)

G. A. Ferguson and Krishnan Raghavachari*

Department of Chemistry, Indiana University, Bloomington, Indiana 47405

David J. Michalak and Yves Chabal

Laboratory for Surface Modification, Rutgers University, Piscataway, New Jersey 08854

Received: July 25, 2007; In Final Form: October 22, 2007

The vibrational spectra of atomically flat hydrogen- and deuterium-passivated Si(111)-(1 × 1) surfaces are investigated using theoretical and experimental techniques. An unexpected isotopic shift is observed for the Si–H bending mode when hydrogen is replaced with deuterium, with $\delta(\text{Si–H}) = 626 \text{ cm}^{-1}$ and $\delta(\text{Si–D}) = 537 \text{ cm}^{-1}$. The Si–H stretching mode, in contrast, behaves as expected with $\nu(\text{Si–H}) = 2083 \text{ cm}^{-1}$ and $\nu(\text{Si–D}) = 1516 \text{ cm}^{-1}$. Density functional studies reveal that the mode observed at 537 cm^{-1} is mostly a phonon mode, which results from the coupling of near-surface phonons with the lower frequency bending mode of the deuterated surface. This coupling causes a shift in the ordering of the expected vibrational modes when hydrogen is replaced by deuterium. We also suggest that such a mode around 535 cm^{-1} should be seen for many other surfaces and is a general feature of many monovalently terminated Si(111) surfaces.

Introduction

Chemical modification of silicon surfaces using organic molecules provides a possible route to highly ordered semiconductor devices containing novel functionality. Much of the current literature^{1–13} in this area has concentrated on functionalization of the Si(111) surface using a two-step alkylation/chlorination technique followed by reaction of the surface with a Grignard reagent.^{14–19} To achieve well-ordered layers, it is necessary to begin with as close to an atomically flat surface as possible. An ideal starting point is the H-passivated Si(111) surface obtained by buffered HF (or NH_4F) etching.²⁰ This process creates an almost atomically flat surface that is ideal for further functionalization described above.^{21–31} The structure of the hydrogen-passivated surface therefore has far-reaching implications for silicon surface functionalization.

Determination of surface structure is a difficult task that is best accomplished using a combination of theory and experiment. In particular, surface infrared vibrational spectroscopy combined with quantum chemical cluster calculations has been used successfully as a probe of surface structure^{3,32} for both Si(100) and Si(111) surfaces. For example, the structure of the methylated Si(111) surface has been determined from HREELS (high-resolution electron energy loss spectroscopy)¹⁸ and surface vibrational spectroscopy¹⁷ and was supported by theoretical calculations.³ The structures of the water dissociation products on Si(100) have also been extensively characterized using a combination of theoretical predictions and experimental observations.³² In many such studies, the structural assignments are confirmed using isotopic substitution reactions, e.g., D_2O substituted for H_2O .³² Using a force constant analysis, it is possible to predict the shift of the hydrogen vibrational modes on deuterium substitution and then confirm the results by observation.

In this work, we have performed vibrational studies using Fourier transform infrared (FTIR) spectroscopy along with gradient-corrected density functional theory and two-dimensional periodic boundary conditions to determine the frequency shifts of deuterated versus hydrogenated Si(111) surfaces. Indeed, the experimental observation of a blue shift of the Si–H bending mode upon deuterium substitution suggests that the nature of the surface vibrational spectrum on such atomically perfect surfaces is more complex than originally thought. The theoretical calculations reveal that, when adsorbate bending vibrations (e.g., the Si–D bending mode) are in the vicinity but lower than selected surface phonon modes, a coupling takes place that substantially affects the surface phonon spectrum. In the case of deuterium, it leads to an increase of a phonon mode at $\sim 537 \text{ cm}^{-1}$, i.e., at a frequency seemingly too high for a pure Si–D bending mode.

Experimental Details

N-type (phosphorus-doped, 24–34 $\Omega \text{ cm}$ resistivity), (111)-oriented, double-side polished, silicon wafers were cut into $\sim 2 \text{ cm} \times 5 \text{ cm}$ pieces for transmission infrared analysis. The native-oxide-terminated samples were first cleaned using the RCA procedure³³ and then etched in 10–20% HF(aq) (30 s) followed by a 2.5 min dip in 40% NH_4F to obtain atomically flat hydrogen-terminated Si(111) samples which were rinsed in H_2O for 10 s.³⁴

D_2O immersion was performed in a Teflon beaker inside a dedicated $\text{N}_2(\text{g})$ -purged flush box. Spectra were recorded first for the native oxide surface and then for a freshly etched H/Si(111) surface; the latter allowed for a comparison of the D/Si(111) surface to the unoxidized H/Si(111) surface. After FTIR analysis, the hydrogen-terminated surface was brought into the $\text{N}_2(\text{g})$ -purged flush box, and the atomically smooth Si–D surface was prepared as reported by Luo and Chidsey.^{35,36}

Anhydrous methanol (CH_3OH , 99.8%), methanol-*d* (CH_3OD , 99+ atom % D), anhydrous methyl-*d*₃ alcohol-*d* (CD_3OD ,

* To whom correspondence should be addressed. E-mail: kraghava@indiana.edu.

99.9+ atom % D), deuterium oxide (D_2O , 99.9 atom % D), anhydrous potassium fluoride (KF, 99.99+%), and deuterium chloride 35 wt % in deuterium oxide (DCl/D_2O , 99 atom % D) were purchased from Aldrich and used as received. Reactions with D_2O -containing solutions were performed in a dedicated nitrogen-purged box, and reactions with methanol were carried out in a separate nitrogen-purged flush box that contained neither D_2O nor H_2O . All H_2O is deionized 18.2 M Ω cm resistivity water from a Millipore system.

Reactions of silicon with methanol were performed at $\sim 65^\circ C$ in (25 \times 150) mm diameter glass tubes. These tubes were initially cleaned with aqua regia, followed by a 10 min clean in a piranha solution, to remove traces of metallic and carbon-containing contamination from the surfaces of the glass. The tubes were then rinsed with H_2O , dried, and brought into a nitrogen glovebox where they were continually reused. Separate tubes were used for acidic H and acidic D species. The tubes were first exposed to $65^\circ C$ anhydrous CH_3OH or anhydrous CH_3OD for at least 30 min to remove traces of H_2O and allow the Si–OH surface of the glass tubes to exchange with the corresponding acidic hydrogen isotope. Reactions were performed in the dark (tubes were wrapped with Al foil) to eliminate reaction pathways involving photogenerated carriers. After the desired reaction time, the solution and sample were poured into a glass funnel, and once dry, the samples were capped in clean tubes under $N_2(g)$ purge, removed from the glovebox, and carried to the spectrometer.

Spectra were recorded in a pyroelectric detector (DTGS) in N_2 -purged Fourier transform infrared spectrometers (Nicolet 6700 and Nexus 670), with 4 cm^{-1} resolution (from 400 to 4000 cm^{-1}) in transmission mode at 74° and 10° incidence. These angles are chosen to be at Brewster angle and close to normal, but avoiding interference effects more pronounced at precisely normal incidence while still providing an electric field essentially parallel to the surface. Five consecutive loops, each consisting of 1000 scans, were obtained for each sample. References were either oxide-terminated or freshly etched hydrogen-terminated surfaces, as appropriate. The absorbance spectra were processed by subtracting water vapor and $CO_2(g)$ peaks and occasionally by baseline corrections to remove drifts.

Computational Details

Surfaces are intrinsically complex systems whose large size and rigid structure present challenges to cluster-based modeling. To overcome these problems, we have used periodic boundary conditions (PBCs) to simulate the effect of an infinite system on a unit cell. The PBC implementation of Kudin and Scuseria,^{37–39} which uses an atom-centered basis function, was used for all energy calculations and geometry optimizations.

As previously mentioned the ground-state structure of the hydrogen- or deuterium-passivated Si(111) surface is the bulk structure with a single adsorbate atom per surface dangling bond.²⁰ This simple structure reduces the number of atoms in the unit cell to one unique atom per layer. It is thus possible to use a larger number of layers to model the system. In our case we have used 10 layers in addition to the upper and lower surface adsorbate atoms, resulting in 12 atoms per unit cell, Figure 1. The model was then completely optimized without constraints using the gradient-corrected BLYP density functional (composed of the B88 exchange functional⁴⁰ and the Lee–Yang–Parr correlation functional⁴¹) with the 6-31G(d,p)⁴²-polarized double- ζ basis set. While hybrid functionals such as B3LYP that include exact exchange are generally more accurate than their GGA counterparts, they are far less cost-effective for

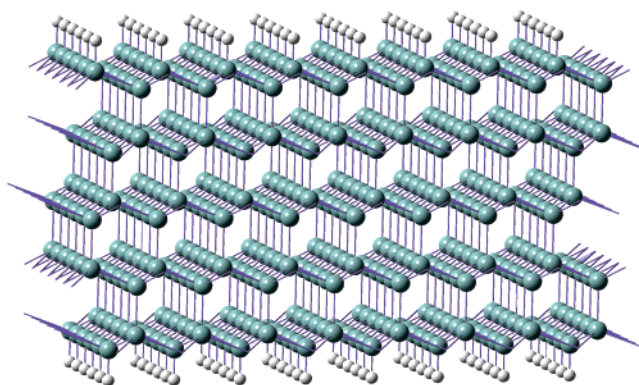


Figure 1. Ten-layer two-dimensional PBC model of the H-terminated Si(111) surface with the larger spheres representing silicon atoms and the small spheres representing hydrogen atoms.

periodic systems of this type. We have shown in previous studies that the BLYP/6-31G(d,p) model provides a reliable description of the vibrational properties for these similar systems.^{3,23}

There are no readily available analytic second derivatives for PBC. Therefore, to calculate the harmonic vibrational frequencies, the analytically obtained forces were numerically differentiated using symmetric displacements of the Cartesian coordinates with a step size of 0.001 \AA . This procedure results in a Cartesian force constant matrix which is then mass-weighted and diagonalized to obtain the vibrational frequencies (eigenvalues) and normal modes (eigenvectors). The resulting frequencies are fully periodic but do not include phonon dispersions, resulting in Γ -point-only frequencies. The consequences of this approximation have been previously described.³ Assignments were then made using these computed vibrational frequencies without any other corrections. All calculations were performed using a modified version of the Gaussian Development Version suite of programs.⁴³

Results and Discussion

The geometry of the hydrogen-passivated Si(111) surface is simple in form. While the structure of the unpassivated Si(111) surface is a complex 7×7 reconstruction under ultra-high-vacuum conditions, hydrogen passivation from a wet-chemical preparation results in the formation of a nearly perfect 1×1 monolayer on the surface²⁰ with a hydrogen atom satisfying the single dangling bond present at each surface silicon. The PBC geometry optimization was accomplished using the BLYP functional, which has given reliable geometries in past studies.^{3,23} It should be noted the bond distances from the BLYP optimized geometry (2.40 \AA for the Si–Si distance and 1.50 \AA for Si–H) are slightly longer than the observed values (e.g., the bulk value silicon–silicon distance is 2.35 \AA). This 2% increase in bond length has been previously discussed.³

It is expected that if a hydrogen atom is replaced with a deuterium, the associated vibrational frequencies will shift to lower values on the basis of the difference in the reduced mass of the total atoms participating in the vibrational mode. Under the approximation that the potential energy surface does not change with isotopic substitution, the nature of the shift for modes that are dominated by hydrogen motion can be predicted by taking the square root of the ratio of the masses, i.e., $1/\sqrt{2}$, or approximately 0.707, for hydrogen to deuterium. This result is expected for both the Si–H stretch and the Si–H bend due to the light mass of hydrogen. The actual shift may vary slightly due to the influence of cubic and quartic terms in the potential energy as well as the contribution of other heavier atoms in the

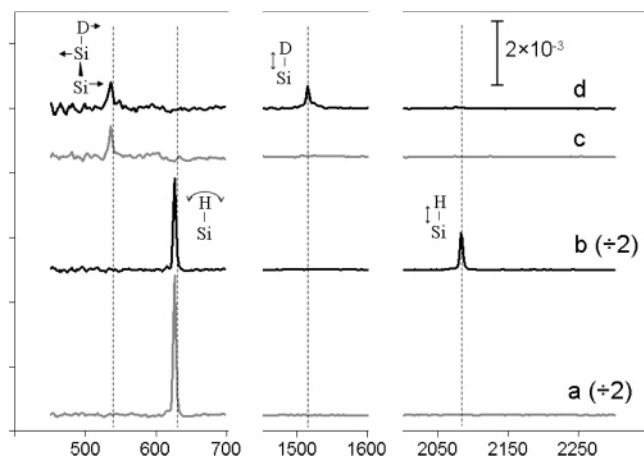


Figure 2. FTIR spectra of the atomically smooth H/Si(111) surface with an infrared-light incidence angle of (a) 10° or (b) 74° off normal and the atomically smooth D/Si(111) surface with an incidence angle of (c) 10° or (d) 74° off normal. For clarity, the intensities of spectra a and b have been divided by a factor of 2 relative to the scale provided.

TABLE 1: Experimental and Calculated Values for the Infrared Vibrational Mode of the Hydrogen- and Deuterium-Terminated Si(111) Surface (cm^{-1})

mode	Si-H, calcd	Si-H, obsd	Si-D, expected ^a	Si-D, calcd	Si-D, obsd
stretching	2120	2083	1499	1525	1516
bending	628	626	444	412	n/o ^c
coupling	476 ^b	n/o	n/o	519	537

^a The expected values are calculated by multiplying the observed Si-H values by $1/\sqrt{2}$ (~ 0.707). ^b The hydrogen-phonon coupling is weak and can be considered almost a pure phonon mode. For this reason, there is very little change in either the intensity or the frequency of this mode for the H/Si(111) or O_x/Si(111) surfaces, and hence, no difference in absorption is observed. ^c n/o stands for not observed out of the noise.

vibration. Using these values, the predicted isotopic shifts are a validation of the surface spectral assignments.

The infrared absorption spectra of H- and D-terminated Si(111)-(1 × 1) shown in Figure 2 confirm that the Si-H stretch mode ($\nu_{\text{Si-H}} = 2084 \text{ cm}^{-1}$) detectable with 74° incidence (spectrum b) and the Si-H bend ($\delta_{\text{Si-H}} = 626 \text{ cm}^{-1}$) detectable with 10° incidence are polarized perpendicular and parallel to the surface, respectively. With near-normal incidence ($\sim 10^\circ$), the electric field is essentially parallel to the surface and therefore cannot excite perpendicular modes, such as the Si-H stretch. Upon deuteration of the Si(111)-(1 × 1) surface, the Si-D stretch is observed at 1514 cm^{-1} (Figure 2d) as expected. However, a strong and sharp mode is also observed at 537 cm^{-1} (Figure 2c,d), well above the expected Si-D bending mode ($\sim 450 \text{ cm}^{-1}$). The theoretical assignment of the modes for the hydrogen- and deuterium-terminated surface is shown in Table 1, with schematics of the modes drawn in Figure 3. While all surface phonon modes were inspected, *only those modes that have a non-negligible (displacement less than $0.1 \text{ amu}^{1/2} \text{ bohr}$) contribution from the hydrogen/deuterium* are listed. The calculated hydrogen stretching mode is seen at 2120 cm^{-1} in the calculated spectrum. The higher-than-expected accuracy of the theoretical value relative to the experimentally observed value can be attributed partly to the cancellation of the opposing effects of anharmonicity and bond length overestimation. The deuterium spectrum is shifted to 1514 cm^{-1} in the experimental spectrum (Figure 2a) and 1525 cm^{-1} in the theoretical spectrum (Table 1, diagram in Figure 3a). The Si-D experimental stretching mode is seen only for an incidence angle of 74°

(Figure 2d) and not for 10° (Figure 2c), so the deuterated surface must be atomically flat with a monodeuteride termination. The experimentally observed frequency of the Si-D stretch is slightly red-shifted relative to previous measurements for an atomically smooth D/Si(111) surface.³⁵ This red shifting implies the presence of some surface-bound impurities that reduce the dipole coupling between neighboring Si-D species.^{35,44–46} The FTIR spectra of our D/Si(111) sample also demonstrate the presence of a small amount of oxidation (approximately 3% of the Si-O-Si longitudinal optical and transverse optical mode areas observed after an SC1/SC2 clean of the native oxide surface) relative to the initial oxide-free H/Si(111) surface. This finding is consistent with this reduction in dipole coupling. The observed Si-D stretching frequencies are very close to the expected shift from simple mass arguments, which are 1499 and 1473 cm^{-1} on the basis of the calculated and experimental frequencies for Si-H, respectively. All these observations are consistent with the well-understood behavior associated with the silicon-hydrogen stretching mode at 2083 cm^{-1} .

The bending mode is both more complicated to assign and more interesting. The experimental value for the hydrogen bending mode has been assigned at 626 cm^{-1} . The dipole for the Si-H bending motion is oriented parallel to the surface and is, hence, observed at both angles of incidence. The assignment is consistent with the calculated value of 628 cm^{-1} . While the computed errors for bending modes are typically smaller, the nearly perfect agreement in this case results from a fortuitous cancellation of the inherent error of the BLYP functional with the neglect of anharmonicity. At first glance the deuterium spectrum gives puzzling results. The expected shift by a factor of approximately 0.707 places the vibration inside the phonon region at 444 cm^{-1} where it may not be easily experimentally observed due to detector limitations. However, a clearly observed feature at 537 cm^{-1} (Figures 2 and 4) is observed at both 74° and 10° off normal, implying that the mode is oriented parallel to the surface. If this peak corresponds to the deuterium bending, it would indicate the vibrational frequency decreases *far less* than expected. Since this occurrence is rather unlikely, we investigated the possibility the mode is not the deuterium bending mode. Considering that the surface has few defects, there are a limited number of other possibilities. For example, the surface may also contain phonon modes that have significant intensity. However, since the observed absorbance spectrum is the difference of two single beam spectra, the phonon modes should be the same in each surface and would be expected to cancel. If it is a phonon mode, it must therefore be a mode of significantly different intensity relative to that of the H/Si(111) or O_x/Si(111) reference surface. Another possibility is the coupling of the deuterium bending mode with the near-surface phonon modes. This phenomenon (i.e., coupling of near-surface phonons with surface adsorbate atoms) has been seen in several previous studies.^{3,23} For this mechanism to be in accordance with the data, the coupling of the near-surface phonon modes with the adsorbate bending must change with the mass change.

When the normal modes (eigenvectors) of the calculated deuterium adsorbate spectrum are examined in the lower frequency region, the deuterium bending mode is seen at 412 cm^{-1} , relatively close to the expected value of 444 cm^{-1} . This mode is dominated by deuterium motion ($\sim 90\%$) with only a modest vibrational coupling with the phonons in this region of the spectrum. This is clearly analogous to the hydrogen bending mode calculated at 628 cm^{-1} (Table 1, diagram in Figure 3b) and observed at 626 cm^{-1} . This mode is clearly *not* the mode that corresponds to the observed mode at 537 cm^{-1} . A closer

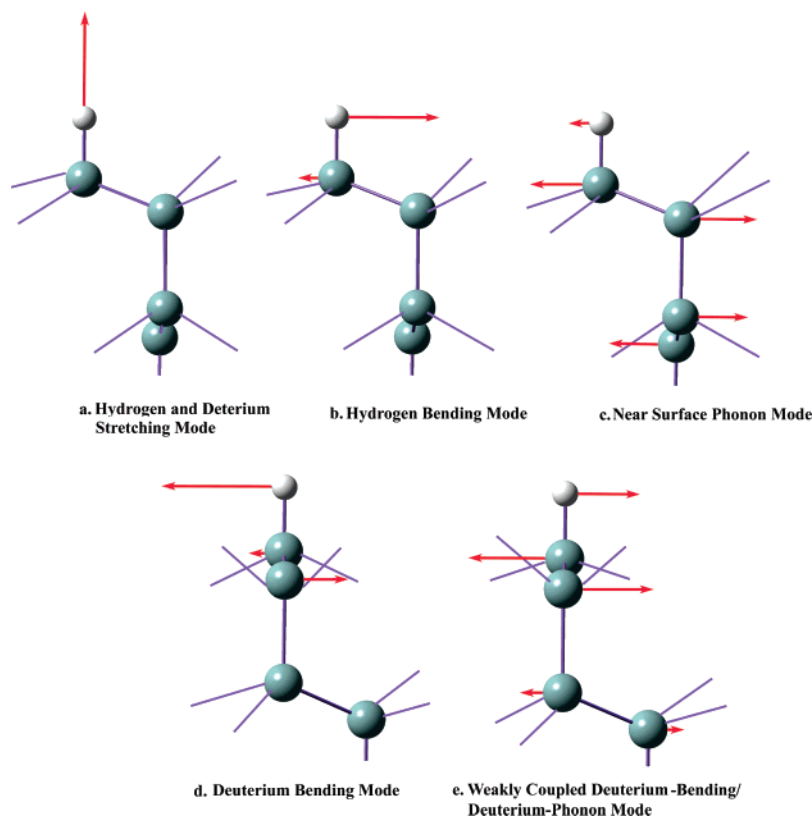


Figure 3. Schematic of the local atomic motions in the key vibrations considered in this study. The atomic displacements (indicated by the length of the arrows) are scaled relative to one another.

inspection of the computed frequencies reveals the presence of another mode at 519 cm^{-1} (Table 1, diagram in Figure 3e) that corresponds to weak coupling between the near-surface phonons and the deuterium bending. Unlike the mode at 412 cm^{-1} (Table 1, diagram in Figure 3d), this mode is mostly dominated by the opposing motion of the first two layers of silicon atoms with a significantly smaller contribution of deuterium bending motion and is polarized parallel to the surface (as observed experimentally). There is a weaker contribution of the deeper silicon layers. A similar phonon mode can also be seen for hydrogen at 476 cm^{-1} (Table 1, diagram in Figure 3c) although the coupling to the hydrogen-bend motion is significantly weaker. It is clear that the coupling is stronger for deuterium, resulting in a higher intensity for deuterium, making it observable for the latter.

We suggest the following explanation for the observations. In the case of deuterium, the intrinsic deuterium bending mode (expected around 440 cm^{-1} , Table 1) is slightly lower in frequency than the intrinsic near-surface phonon mode that occurs around $480\text{--}500\text{ cm}^{-1}$. The coupling to the phonon from the lower frequency Si–D bend shifts the phonon mode to higher frequency (computed at 519 cm^{-1} , Table 1, diagram in Figure 3e) and allows it to be detectable. In the case of hydrogen, the intrinsic bending mode ($\sim 620\text{ cm}^{-1}$, Table 1, diagram in Figure 3b) is significantly higher in frequency than the near-surface phonon modes. The coupling is much weaker due to the lighter mass of hydrogen as well as the larger intrinsic frequency difference and shifts the phonon mode slightly lower in frequency.

Overall, in the case of hydrogen, the observed mode at 626 cm^{-1} is mostly composed of Si–H bending, while in the case of deuterium, the observed mode at 537 cm^{-1} is mostly composed of phonon motion. The differences arise from the fact that, on going from H to D, the intrinsic bend moves from *above* the phonon region to *below* the phonon region. Our

computational studies show that the point at which the qualitative nature of the mode changes, i.e., the point at which the intrinsic modes are equal in frequency, occurs for adsorbate atoms having masses around 1.6 amu.

The observation of such an adsorbate-coupled near-surface phonon mode can also be seen for the chlorine-terminated surface at 527 cm^{-1} and for the methyl-terminated surface at 522 cm^{-1} .³ The intrinsic bending mode for both of these adsorbates is also lower in frequency than the intrinsic phonon mode. The fact that the mode shifts only slightly with the adsorbate (e.g., D vs Cl) is consistent with a mode composed mostly of a phonon whose frequency blue shifts slightly, but sufficiently high enough, with different adsorbate atoms to be observable. We predict that a similar mode is likely to be seen for other monovalent adsorbates on the unreconstructed Si(111)-(1 × 1) surface with a mass greater than that of deuterium. From this combined theoretical and experimental evidence, we can assign the 537 cm^{-1} mode of the D/Si(111) surface to near-surface phonons weakly coupled to the deuterium bending mode. If it is possible to examine the spectrum at lower frequencies, we believe the deuterium bending mode would appear around 400 cm^{-1} , as expected. Unfortunately, no reliable information can be obtained below 460 cm^{-1} , due to detector response and beamsplitter efficiency, making it impossible with our current spectrometer system to explore the true Si–D bending mode. Nevertheless, these observations confirm that the simple isotopic exchange from hydrogen to deuterium leads to a considerable difference in the degree of coupling between the subsurface phonons and the surface adsorbates.

Figure 4 demonstrates that the Si–D coupled phonon and bending mode can be observed for other Si–D-containing surfaces even when it is dispersed among different adsorbate species. The spectra in Figure 4 result from the exposure of atomically smooth H/Si(111) to $65\text{ }^\circ\text{C}$ solutions of neat

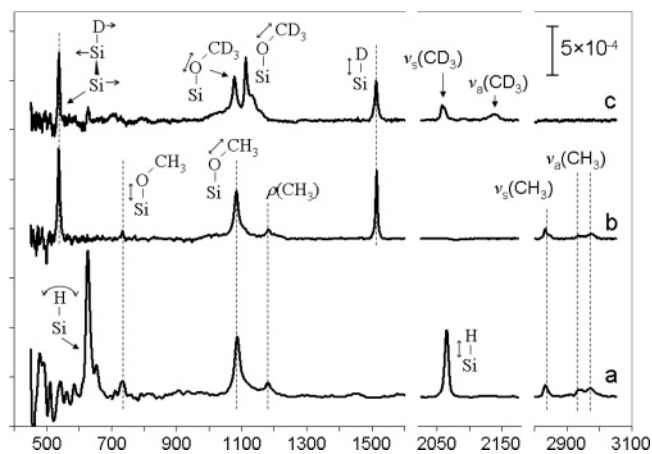


Figure 4. FTIR spectra for H/Si(111) surfaces after a 3 h exposure to a 65 °C solution of (a) CH₃OH, (b) CH₃OD, or (c) CD₃OD. Reaction with CH₃OH or CH₃OD produced similar amounts of surface-bound Si-OCH₃ species (i.e., similar peak areas were observed for the CH₃ stretching modes at 2832, 2940, and 2970 cm⁻¹, for the CH₃ umbrella modes at 1190 cm⁻¹, for the modes at 1085 cm⁻¹, which are comprised of a C-O stretch coupled with a CH₃ bending motion, and for the Si-O stretching modes at 735 cm⁻¹). The Si-H stretching (2083.7 cm⁻¹) and Si-H bending (626 cm⁻¹) modes were, however, only observed on surfaces reacted with CH₃OH. For surfaces reacted with either CH₃OD or CD₃OD, no detectable Si-H modes were observed, and only the Si-D mode (1512 cm⁻¹) and Si-Si-D coupled phonon and bending mode (537 cm⁻¹) were observed. The isotopic exchange of the remaining Si-H sites (approximately 70% of a monolayer) after reaction with either CH₃OD or CD₃OD has been observed previously³¹ and is ascribed to either a step-flow or a direct-exchange mechanism. Reaction of H/Si(111) with CD₃OD produces a similar amount of Si-D surface coverage relative to CH₃OD, but spectral features attributing to the formation of Si-OCD₃ sites are observed (CD₃ stretching peaks at 2068, 2216, and 2224 cm⁻¹, a coupled CD₃ umbrella and C-O stretching mode at 1112 cm⁻¹, a coupled Si-O-C stretch and a CD₃ bending mode at 1078 cm⁻¹, and Si-O stretching peaks at 735 cm⁻¹). Very little observable subsurface oxidation was observed after any of these reactions. For clarity, the spectral regions of 450–700 and 2000–2200 cm⁻¹ have been referenced relative to the native oxide surface, while the spectral regions of 700–1600 and 2800–3050 cm⁻¹ have been referenced relative to the freshly etched H/Si(111) surface.

anhydrous CH₃OH, CH₃OD, and CD₃OD. In these cases, approximately 30% of the initial Si-H is removed and replaced with either Si-OCH₃ or Si-OCD₃. This replacement occurs randomly across the surface, rather than in phase-separated domains, on the basis of the red shift in the Si-H stretching mode.³¹ The surfaces that result from this chemistry retain their initial atomically smooth nature as evidenced by the orientation of the resulting modes (both Si-OCH₃- and Si-H-related) and the absence of any detectable dihydride or monohydride step modes. Despite the difference in chemistry of the surface sites (70% Si-D and ~30% Si-OCH₃ or Si-OCD₃), the coupled Si-D bending and near-surface phonon modes are almost the same intensity relative to those of the smooth deuterated surface (vide supra). The fact that the coupling of the intrinsic bending modes of the surface adsorbates to the phonon mode does not shift with surface coverage was also seen in our computational studies of small clusters when one of the seven surface deuterium atoms was replaced with a methyl group. Since the mode is mostly comprised of phonon motion that is weakly coupled to the surface adsorbate, it can be understood that it may not shift significantly due to relatively minor surface-coverage changes in the adsorbate atoms. For this to be the case, the splitting between the near-surface phonon mode coupled to a deuterium or methyl adsorbate should not be large, in accordance with the observed spectra. In the future, it will be

interesting to explore the nature of such vibrational interactions as a function of surface coverage and surface disorder and for other more complex adsorbates.

Conclusions

To summarize, we have investigated the spectrum of the deuterated and hydrogen-terminated Si(111) surface using theoretical and experimental techniques. To explain the unexpected presence of a sharp vibrational mode around 535 cm⁻¹ for deuterated, chlorinated, and methylated Si(111)-(1 × 1) surfaces, it was necessary to consider the coupling of near-surface phonons with the bending mode of the surface. This phenomenon resulted in a shift in the ordering of the expected vibrational modes when hydrogen was replaced by deuterium. We have assigned the vibrational modes of both surfaces and have offered a simple explanation for the appearance of this phonon mode on Si(111)-(1 × 1) surfaces containing adsorbates heavier than hydrogen.

Acknowledgment. We acknowledge NSF Grant CHE-0616737 at Indiana University and NSF Grant CHE-0415652 at Rutgers University for financial support.

Supporting Information Available: Entire FTIR spectral window of Figures 2 and 4. This material is available free of charge via the Internet at <http://pubs.acs.org>.

References and Notes

- Bent, S. F. *Surf. Sci.* **2002**, *500* (1–3), 879.
- Bent, S. F. *J. Phys. Chem. B* **2002**, *106* (11), 2830.
- Ferguson, G.; Raghavachari, K. *J. Chem. Phys.* **2006**, *125* (15), 154708.
- Filler, M. A.; Bent, S. F. *Prog. Surf. Sci.* **2003**, *73* (1–3), 1.
- Haber, J. A.; Lauermaun, I.; Michalak, D.; Vaid, T. P.; Lewis, N. S. *J. Phys. Chem. B* **2000**, *104* (43), 9947.
- Haick, H.; Hurley, P. T.; Hochbaum, A. I.; Yang, P.; Lewis, N. S. *J. Am. Chem. Soc.* **2006**, *128*, 8990.
- Hunger, R.; Fritsche, R.; Jaeckel, B.; Jaegermann, W.; Webb, L. J.; Lewis, N. S. *Phys. Rev. B* **2005**, *72* (4), 045317.
- Linford, M. R.; Chidsey, C. E. D. *Langmuir* **2002**, *18* (16), 6217.
- Lopinski, G.; Wayner, D.; Wolkow, R. *Nature* **2000**, *406*, 48.
- Rivillon, S.; Chabal, Y. J. *J. Phys. Chem. B* **2006**, *132*, 195.
- Solares, S. D.; Michalak, D. J.; Goddard, W. A.; Lewis, N. S. *J. Phys. Chem. B* **2006**, *110* (16), 8171.
- Sze, S. M. *The Physics of Semiconductor Devices*, 2nd ed.; Wiley-Interscience: New York, 1981.
- Yates, J. T. *Science* **1998**, *279* (5349), 335.
- Bansal, A.; Li, X. L.; Yi, S. I.; Weinberg, W. H.; Lewis, N. S. *J. Phys. Chem. B* **2001**, *105* (42), 10266.
- Hurley, P. T.; Nemanick, E. J.; Brunschwigg, B. S.; Lewis, N. S. *J. Am. Chem. Soc.* **2006**, *128*, 9990.
- Webb, L. J.; Lewis, N. S. *J. Phys. Chem. B* **2003**, *107* (23), 5404.
- Webb, L. J.; Rivillon, S.; Michalak, D. J.; Chabal, Y. J.; Lewis, N. S. *J. Phys. Chem. B* **2006**, *110* (14), 7349.
- Yamada, T.; Kawai, M.; Wawro, A.; Suto, S.; Kasuya, A. *J. Chem. Phys.* **2004**, *121* (21), 10660.
- Yu, H. B.; Webb, L. J.; Ries, R. S.; Solares, S. D.; Goddard, W. A.; Heath, J. R.; Lewis, N. S. *J. Phys. Chem. B* **2005**, *109* (2), 671.
- Higashi, G. S.; Chabal, Y. J.; Trucks, G. W.; Raghavachari, K. *Appl. Phys. Lett.* **1990**, *56* (7), 656.
- Linford, M. R.; Fenter, P. P.; Eisenberger, M.; Chidsey, C. E. D. *J. Am. Chem. Soc.* **1995**, *117* (11), 3145.
- Nemanick, E. J.; Hurley, P. T.; Webb, L. J.; Knapp, D. W.; Michalak, D. J.; Brunschwigg, B. S.; Lewis, N. S. *J. Phys. Chem. B* **2006**, *110* (30), 14770.
- Rivillon, S.; Chabal, Y. J.; Webb, L. J.; Michalak, D. J.; Lewis, N. S.; Halls, M. D.; Raghavachari, K. *J. Vac. Sci. Technol., A* **2005**, *23* (4), 1100.
- Rohde, R. D.; Agnew, H. D.; Yeo, W.; Bailey, R. C.; Heath, J. R. *J. Am. Chem. Soc.* **2006**, *128*, 9518.
- Solares, S. D.; Yu, H. B.; Webb, L. J.; Lewis, N. S.; Heath, J. R.; Goddard, W. A. *J. Am. Chem. Soc.* **2006**, *128* (12), 3850.
- Takeuchi, N.; Kanai, Y.; Selloni, A. *J. Am. Chem. Soc.* **2004**, *126* (48), 15890.

- (27) Terry, J.; Linford, M. R.; Wigren, C.; Cao, R. Y.; Pianetta, P.; Chidsey, C. E. D. *Appl. Phys. Lett.* **1997**, *71* (8), 1056.
- (28) Terry, J.; Linford, M. R.; Wigren, C.; Cao, R. Y.; Pianetta, P.; Chidsey, C. E. D. *J. Appl. Phys.* **1999**, *85* (1), 213.
- (29) Webb, L. J.; Nemanick, E. J.; Biteen, J. S.; Knapp, D. W.; Michalak, D. J.; Traub, M. C.; Chan, A. S. Y.; Brunschwig, B. S.; Lewis, N. S. *J. Phys. Chem. B* **2005**, *109* (9), 3930.
- (30) Yamada, T.; Inoue, T.; Yamada, K.; Takano, N.; Osaka, T.; Harada, H.; Nishiyama, K.; Taniguchi, I. *J. Am. Chem. Soc.* **2003**, *125* (26), 8039.
- (31) Michalak, D. J.; Rivillon, S.; Chabal, Y. J.; Esteve, A.; Lewis, N. S. *J. Phys. Chem. B* **2006**, *110* (41), 20426.
- (32) Raghavachari, K. Y.; Chabal, Y. J.; Struck, L. M. *Chem. Phys. Lett.* **1996**, *252* (3–4), 230.
- (33) This procedure involved a 10 min exposure to an 80 °C solution of 4:1:1 H₂O/30% H₂O₂(aq)/concentrated NH₄OH(aq), a H₂O rinsing step, a 10 min exposure to an 80 °C solution of 4:1:1 H₂O/30% H₂O₂(aq)/concentrated HCl(aq), and a final H₂O rinsing step.
- (34) Chabal, Y. J.; Hines, M. A.; Feijoo, D. *J. Vac. Sci. Technol., A* **1995**, *13* (3), 1719.
- (35) Luo, H. H.; Chidsey, C. E. D. *Appl. Phys. Lett.* **1998**, *72* (4), 477.
- (36) Briefly, 0.5 mL of 35% DCl in D₂O was added to a solution containing ~5 g of anhydrous KF in ~30 mL of D₂O. The H/Si(111) sample was immersed in the solution for 5 min and was dry and clean when lifted out of the solution. The sample was briefly rinsed with D₂O, blown dry with N₂(g), and capped in a centrifuge tube for transport to the spectrometer (<2 min).
- (37) Ayala, P. Y.; Kudin, K. N.; Scuseria, G. E. *J. Chem. Phys.* **2001**, *115* (21), 9698.
- (38) Kudin, K. N.; Scuseria, G. E. *Chem. Phys. Lett.* **1998**, *289* (5–6), 611.
- (39) Kudin, K. N.; Scuseria, G. E.; Schlegel, H. B. *J. Chem. Phys.* **2001**, *114* (7), 2919.
- (40) Becke, A. D. *Phys. Rev. A* **1988**, *38* (6), 3098.
- (41) Lee, C. T.; Yang, W. T.; Parr, R. G. *Phys. Rev. B* **1988**, *37* (2), 785.
- (42) Harihara, P.; Pople, J. A. *Theor. Chim. Acta* **1973**, *28* (3), 213.
- (43) Frisch, M. J.; Trucks, G. W.; Schlegel, H. B.; Scuseria, G. E.; Robb, M. A.; Cheeseman, J. R.; Montgomery, J. J. A.; Vreven, T.; Kudin, K. N.; Burant, J. C.; Millam, J. M.; Iyengar, S. S.; Tomasi, J.; Barone, V.; Mennucci, B.; Cossi, M.; Scalmani, G.; Rega, N.; Petersson, G. A.; Nakatsuji, H.; Hada, M.; Ehara, M.; Toyota, K.; Fukuda, R.; Hasegawa, J.; Ishida, M.; Nakajima, T.; Honda, Y.; Kitao, O.; Nakai, H.; Klene, M.; Li, X.; Knox, J. E.; Hratchian, H. P.; Cross, J. B.; Bakken, V.; Adamo, C.; Jaramillo, J.; Gomperts, R.; Stratmann, R. E.; Yazyev, O.; Austin, A. J.; Cammi, R.; Pomelli, C.; Ochterski, J. W.; Ayala, P. Y.; Morokuma, K.; Voth, G. A.; Salvador, P.; Dannenberg, J. J.; Zakrzewski, V. G.; Dapprich, S.; Daniels, A. D.; Strain, M. C.; Farkas, O.; Malick, D. K.; Rabuck, A. D.; Raghavachari, K.; Foresman, J. B.; Ortiz, J. V.; Cui, Q.; Baboul, A. G.; Clifford, S.; Cioslowski, J.; Stefanov, B. B.; Liu, G.; Liashenko, A.; Piskorz, P.; Komaromi, I.; Martin, R. L.; Fox, D. J.; Keith, T.; Al-Laham, M. A.; Peng, C. Y.; Nanayakkara, A.; Challacombe, M.; Gill, P. M. W.; Johnson, B.; Chen, W.; Wong, M. W.; Gonzalez, C.; Pople, J. A. *Gaussian Development Version*; Gaussian: Wallingford, CT, 2004.
- (44) Jakob, P.; Chabal, Y. J.; Raghavachari, K. *Chem. Phys. Lett.* **1991**, *187* (3), 325.
- (45) Jakob, P.; Chabal, Y. J.; Raghavachari, K.; Christman, S. B. *Phys. Rev. B* **1993**, *47* (11), 6839.
- (46) Jakob, P.; Chabal, Y. J.; Raghavachari, K.; Dumas, P.; Christman, S. B. *Surf. Sci.* **1993**, *285* (3), 251.